Mineralogical Magazine, December 2014, Vol. 78(7), pp. 1687–1698

Unique thallium mineralization in the fumaroles of Tolbachik volcano, Kamchatka Peninsula, Russia. I. Markhininite, $TlBi(SO_4)_2$

Oleg I. Siidra[1,*], Lidiya P. Vergasova[2], Sergey V. Krivovichev[1,3], Yuri L. Kretser[4], Anatoly N. Zaitsev[5] and Stanislav K. Filatov[1]

[1] Department of Crystallography, St Petersburg State University, University Emb. 7/9, 199034 St Petersburg, Russia
[2] Institute of Volcanology, Russian Academy of Sciences, Bulvar Piypa 9, 683006 Petropavlovsk-Kamchatskiy, Russia
[3] Institute of silicate Chemistry, Russian Academy of Sciences, Makarova Emb. 6, 199034 St Petersburg, Russia
[4] V.G. Khlopin Radium Institute, Roentgen Street 1, 197101 St Petersburg, Russia
[5] Department of Mineralogy, St Petersburg State University, University Emb. 7/9, 199034 St Petersburg, Russia

[*Received 17 March 2014; Accepted 17 June 2014; Associate Editor: P. Leverett*]

ABSTRACT

Markhininite, ideally $TlBi(SO_4)_2$, was found in a fumarole of the 1st cinder cone of the North Breach of the Great Fissure Tolbachik volcano eruption (1975–1976), Kamchatka Peninsula, Russia. Markhininite occurs as white pseudohexagonal plates associated with shcherbinaite, pauflerite, bobjonesite, karpovite, evdokimovite and microcrystalline Mg, Al, Fe and Na sulfates. Markhininite is triclinic, $P\bar{1}$, $a = 7.378(3)$, $b = 10.657(3)$, $c = 10.657(3)$ Å, $\alpha = 61.31(3)$, $\beta = 70.964(7)$, $\gamma = 70.964(7)^{\circ}$, $V = 680.2(4)$ Å^3, $Z = 4$ (from single-crystal diffraction data). The eight strongest lines of the X-ray powder diffraction pattern are (*I*/*d*/*hkl*): 68/4.264/111, 100/3.441/113, 35/3.350/222, 24/3.125/122, 23/3.054/202, 45/2.717/022, 20/2.217/331, 34/2.114/204. Chemical composition determined by electron microprobe analysis is (wt.%): Tl_2O 35.41, Bi_2O_3 38.91, SO_3 25.19, total 99.51. The empirical formula based on 8 O a.p.f.u. is $Tl_{1.04}Bi_{1.05}S_{1.97}O_8$. The simplified formula is $TlBi(SO_4)_2$, which requires Tl_2O 35.08, Bi_2O_3 38.48, SO_3 26.44, total 100.00 wt.%. The crystal structure was solved by direct methods and refined to $R1 = 0.055$ on the basis of 1425 independent observed reflections. The structure contains four Tl^+ and two Bi^{3+} sites in holodirected symmetrical coordination. BiO_8 tetragonal antiprisms and SO_4 tetrahedra in markhininite share common O atoms to produce $[Bi(SO_4)_2]^-$ layers of the yavapaiite type. The layers are parallel to (111) and linked together through interlayer Tl^+ cations. The mineral is named in honour of Professor Yevgeniy Konstantinovich Markhinin (b. 1926), Institute of Volcanology, Russian Academy of Sciences, Kamchatka peninsula, Russia, in recognition of his contributions to volcanology. Markhininite is the first oxysalt compound that contains both Tl and Bi in an ordered crystal structure.

Keywords: markhininite, new mineral, thallium, bismuth, sulfates, layered structures, yavapaiite-type compounds, Tolbachik volcano.

Introduction

Thallium (Tl) is an exceptionally rare element in both mantle and crustal rocks. Its concentration in the Earth's mantle is estimated as 3 ppb, the bulk continental crust contains 360 ppb of Tl (900 ppb in the upper continental crust), and the element shows the highest degree of enrichment in the crust over the mantle compared to all other elements (Palme and O'Neill, 2003; Rudnick and Gao, 2003 and references therein). Much higher

* E-mail: o.siidra@spbu.ru
DOI: 10.1180/minmag.2014.078.7.12

Tl concentrations are known for marine sediments – 1.8, 4.8, 34 and 150 ppm for pelagic clays, basal and ridge sediments, and Fe-Mn nodules, respectively (Li and Schoonmaker, 2003 and references therein). Depending on the chemical environment, thallium could exhibit either lithophile or chalcophile behaviour; the former results in substitution of potassium in rock-forming minerals and the latter leads to the formation of Tl-bearing minerals.

Fifty-three thallium minerals are known to date and the majority of these are sulfides and sulfosalts (CNMNC, 2013). Thallium minerals *sensu stricto* (i.e. minerals with independent crystallographic positions dominated by Tl) occur mainly in rocks of hydrothermal origin associated with epithermal and mesothermal polymetallic deposits (Johan and Mantienne, 2000) and alkaline to peralkaline rocks (Karup-Møller and Makovicky, 2011). Thallium minerals are also known from magmatic sulfide ores associated with ultrabasic rocks (Kovalenker *et al*., 1976) and their oxidation zones (Balić-Žunić *et al*., 1994; Daiyan *et al*., 2001).

Studies of gases from active volcanic areas, such as Italy, Java, Hawaii and New Zealand, show enrichment in thallium owing to the highly volatile behaviour of the element at high and medium temperatures during magma degassing (Baker *et al*., 2009; Prytulak *et al*., 2013). High Tl concentrations are even used as a tracer for pre-industrial volcanic eruptions (Kellerhals *et al*., 2010). Recently, three new Tl minerals have been discovered in the high-temperature fumaroles of the La Fossa crater, Vulcano Island, Italy (Roberts *et al*., 2006; Campostrini *et al*., 2008; Demartin *et al*., 2009).

The Great Tolbachik Fissure eruption (GTFE) that occurred in 1975–1976 on Kamchatka Peninsula, Russia (Fedotov, 1984), was followed by exceptional fumarolic activity and formation of many unique assemblages of mineral species. More than 40 new minerals have been discovered at this locality so far, including sulfates, arsenates, selenites, chlorides, vanadates, etc. [For recent discoveries see Zelenski *et al*. (2011, 2012), Pekov *et al*. (2012*a*,*b*, 2013*a*,*b*), Starova *et al*. (2012), Krivovichev *et al*. (2013*a*), Murashko *et al*. (2013) and Shuvalov *et al*. (2013)]. Relatively large concentrations of thallium have been reported in Tolbachik basalts and metasomatic rocks formed as a result of interactions of basalts with fumarolic gases by Naboko and Glavatskikh (1984). The maximum content of Tl in the 2nd cinder cone of the GTFE was reported as 77 ppm, whereas, in the 1st cinder cone it was reported as being up to 18 ppm. However, no Tl minerals from the Tolbachik volcano have been reported so far. Thallium enrichment of fumarolic gases at Tolbachik might be explained by subduction of Tl-bearing marine sediments and the Pacific oceanic plate under Kamchatka with subsequent magma degassing (Baker *et al*., 2009, Prytulak *et al*., 2013).

A recent investigation of Tolbachik samples collected from fumaroles in 1977 led to the discovery of three new thallium sulfate and vanadyl-sulfate minerals, which are reported in this and two subsequent publications (Siidra *et al*., 2014*a*,*b*). Herein we report the composition, structure and properties of markhinite, $TlBi(SO_4)_2$, the first Tl and Bi sulfate. The mineral is named in honour of Professor Yevgeniy Konstantinovich Markhinin (b. 1926), Institute of Volcanology, Russian Academy of Sciences, Kamchatka Peninsula, Russia, in recognition of his contributions to volcanology. Professor Markhinin has studied dozens of volcanoes, volcanic eruptions and their geochemistry and developed a method for determination of the chemical composition of fumarolic gases [see, e.g. Markhinin (1967) and Fedotov and Markhinin (2011)]. Both the mineral and the mineral name were approved by the Commission on New Minerals, Nomenclature and Classification of the International Mineralogical Association (proposal 2012-040, Filatov *et al*, 2013). Type material is deposited in the Mineralogical Museum, St Petersburg State University, St Petersburg, Russia, catalogue number 1/19526.

Occurrence and association

Markhininite occurs as a product of fumarolic activity. It was found in fumaroles of the 1st cinder cone of the North breach of the GTFE, Kamchatka Peninsula, Russia (Fig.1). The temperature of gases in the sampling location was ~500ºC. All the samples recovered were packed and isolated to avoid any contact with the atmosphere. Markhininite is associated with shcherbinaite, pauflerite, bobjonesite, karpovite, evdokimovite and microcrystalline Mg, Al, Fe and Na sulfates. The specimen with Tl-rich sulfate mineralization was ~8 cm × 8 cm × 3 cm in size. The specimen was covered by blue bobjonesite, brown to golden shcherbinaite and greenish pauflerite. White transparent crystals of markhininite with a pseudo-hexagonal habit grow on shcherbinaite needles

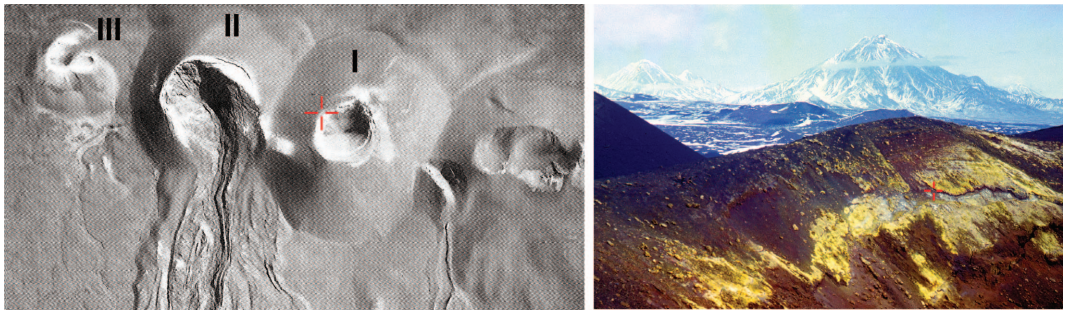

FIG. 1. Location of fumaroles with Tl-rich sulfate mineralization (indicated by red crosses) in the first cinder cone of the North breach of the GFTE, Kamchatka Peninsula, Russia in 1977: aerial view (left) and photo (right). Numbers in the left part of the figure correspond to the numbers of the cinder cones.

(Fig. 2) and form intergrowths with bobjonesite. Other associated minerals are evdokimovite and karpovite (Siidra *et al*., 2014*a*,*b*). No other Bi minerals have been observed in the sample.

Physical properties

Markhininite is white with a white streak and adamantine to translucent lustre. It is brittle with a perfect cleavage on {011}. No parting is observed and fracture is conchoidal. Hardness and density could not be measured due to lack of suitable material. The calculated density for the ideal formula of $TlBi(SO_4)_2$ is 5.91 g cm^{-3}.

Chemical composition

Chemical analyses (20) were performed using a Camscan-4DV scanning electron microscope and an AN-10000 semiconductor spectrometer operating at 20 kV and 1 nA at the V.G. Khlopin Radium Institute, St Petersburg. Tl$L\alpha$, Bi$L\alpha$ and S$K\alpha$, were used as analytical lines. Tl$M\alpha$ and Bi$M\alpha$ lines were subtracted to get the correct chemical formula because of partial overlap with the S$K\alpha$ line. All calculations were made using *AF4/FLS* software. Fe, As, V, P and Si were sought but were below detection limits. No other elements were detected. Analytical data are given in Table 1. The empirical formula based on 8 O atoms per formula unit is $Tl_{1.04}Bi_{1.05}S_{1.97}O_8$. The simplified formula is $TlBi(SO_4)_2$, which requires Tl_2O 35.08, Bi_2O_3 38.48, SO_3 26.44, total 100.00 wt.%.

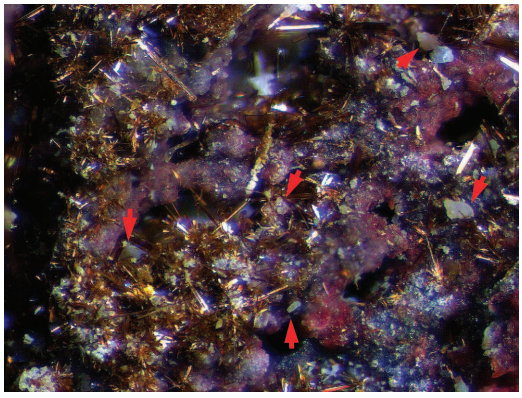

FIG. 2. Red arrows point to the white markhininite plates in a mass of golden yellow needle-like crystals of shcherbinaite. Field of view is ~1.9 mm.

Powder X-ray diffraction data

Powder X-ray diffraction (XRD) data were collected using a Stoe IPDS II diffractometer at the Department of Crystallography, St Petersburg State University, Russia, after crushing the crystal fragment used for the single crystal analysis. Data (in Å for Mo$K\alpha$) are given in Table 2. Unit-cell parameters refined from the powder data are triclinic, space group $P\bar{1}$, a = 7.375(9), b = 10.647(16), c = 10.671(12) Å, α = 61.24(9), β = 70.77(13), γ = 70.85(10)º, V = 679(1) $Å^3$, Z = 4. The eight strongest lines of the XRD pattern are (*I*/*d*/*hkl*): 68/4.264/111, 100/3.441/113, 35/3.350/222, 24/3.125/122, 23/3.054/202, 45/2.717/022, 20/2.217/331, 34/2.114/204.

Crystal structure

Experimental

A small transparent plate-like crystal fragment of markhininite was mounted on a thin glass fibre for XRD analysis using a Bruker APEX II DUO XRD

TABLE 1. Chemical composition (wt.%) of markhininite.

Constituent	wt.%	Range	SD	Probe standard
Tl_2O	35.41	35.38–35.44	0.03	TlI
Bi_2O_3	38.91	38.87–38.93	0.02	Bi metal
SO_3	25.19	25.17–25.21	0.02	Pyrite
Total	99.51			

with a micro-focus X-ray tube operated with Mo$K\alpha$ radiation at 50 kV and 40 mA. Data were integrated and corrected for absorption using a multi-scan model implemented in the Bruker programs *APEX* and *SADABS*. More than a hemisphere of XRD data was collected. Initial indexing of diffraction data indicated a *C*-centred monoclinic cell with the parameters a = 18.335, b = 10.867, c = 7.378 Å, β = 112.281º. However, all attempts to solve the structure in monoclinic space groups corresponding to this unit cell were unsuccessful and led to essential disorder in either Tl or Bi positions. Therefore the structure was solved in the non-standard triclinic space group *C*1 and then transformed into the $P\bar{1}$ space group by *PLATON* (Speck, 2003) through the application of the transformation matrix [−½½0 / −½−½0 / 001] to provide the unit-cell dimensions listed in Table 3. Refinement in $P\bar{1}$ converged to R_1 = 0.102 with no disorder observed for the heavy-atom sites. A twinning matrix [100/001/010] was then applied, which resulted in a decrease of the R_1 value to 0.055. The relations between the pseudo-monoclinic cell, the triclinic cell and the twin plane are shown in Fig. 3. The final model included anisotropic displacement parameters for Bi and Tl atoms. Refinement of the S and O positions in an anisotropic approximation resulted in physically

TABLE 2. X-ray powder diffraction data for markhininite. The eight strongest lines are shown in bold

I_{rel}	d_{obs}	d_{calc}	h	k	l
12	6.682	6.703	1	1	1
8	4.983	5.017	0	$\bar{2}$	$\bar{1}$
68	**4.264**	4.252	1	1	$\bar{1}$
6	3.651	3.688	2	1	1
100	**3.442**	3.436	1	1	3
35	**3.350**	3.352	2	2	2
19	3.222	3.239	0	$\bar{2}$	$\bar{3}$
24	**3.125**	3.113	1	$\bar{2}$	$\bar{2}$
23	**3.054**	3.051	2	0	2
45	**2.717**	2.717	0	$\bar{2}$	2
2	2.467	2.477	0	$\bar{4}$	$\bar{1}$
10	2.283	2.288	0	0	$\bar{4}$
20	**2.217**	2.214	3	3	1
34	**2.114**	2.112	2	0	4
3	1.929	1.932	2	5	1
9	1.855	1.850	3	3	5
13	1.750	1.751	1	3	$\bar{3}$
15	1.678	1.676	4	4	4
8	1.628	1.626	1	5	6
8	1.564	1.566	1	1	$\bar{5}$
6	1.522	1.526	4	4	0
2	1.490	1.492	4	$\bar{2}$	1
5	1.426	1.426	4	6	2

TABLE 3. Crystallographic data and refinement parameters for markhininite.

Crystal size (mm)	0.02 × 0.12 × 0.13
Space group	$P\bar{1}$
a (Å)	7.378(3)
b (Å)	10.657(3)
c (Å)	10.657(3)
α (º)	61.31(3)
β (º)	70.964(7)
γ (º)	70.964(7)
V (Å^3)	680.2(4)
μ (mm^{-1})	50.119
D_{calc} (g cm^{-3})	5.913
Radiation wavelength (Å)	0.71073 (Mo$K\alpha$)
θ range (deg.)	2.23–27.99
Total Ref.	6010
Unique Ref.	2569
Unique $F \geqslant 4\sigma(F)$	1425
R_{int}	0.045
R_1	0.055
R_1 (all data)	0.091
Gof	1.033
$\rho_{max,min}$ (e Å^{-3})	+4.969/−3.566

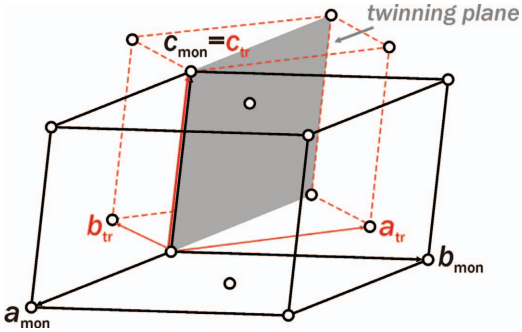

FIG. 3. Relations between pseudo-monoclinic (a_{mon}, b_{mon}, c_{mon}) and triclinic (a_{tr}, b_{tr}, c_{tr}) unit cells and the position of the twin plane in the structure of markhininite.

unrealistic parameters, which can be explained by the effects of twinning and high dominance of strong and diffuse electron configurations of Bi and Tl atoms. These effects also resulted in unreliable S–O bond lengths and very high values of their standard deviations (up to 0.04 Å), which makes bond-valence analysis of the structure non-applicable. Final atom coordinates and anisotropic displacement parameters are given in Table 4 and selected interatomic distances in Table 5. Lists of observed and calculated structure factors have been deposited with the Principal Editor of *Mineralogical Magazine* and are available from www.minersoc.org/pages/e_journals/dep_mat_mm.html.

Cation coordination

The structure of markhininite contains four Tl^{+} and two Bi^{3+} sites. All thallium atoms demonstrate similar coordination which can be described as a combination of a distorted hexagonal pyramid and prism (Fig. 4). Each of the four Tl^{+} cations forms 14 Tl–O bonds with bond lengths in the range 3.01–3.50 Å (Table 5). The coordination spheres of Tl^{+} in markhininite are characterized by a rather uniform distribution of shorter and stronger bonds and can be described as "holodirected"

TABLE 4. Atom coordinates and displacement parameters (Å^2) for markhininite.

Atom	*x/a*	*y/b*	*z/c*	U_{eq}	U^{11}	U^{22}	U^{33}	U^{23}	U^{13}	U^{12}
Bi1	−0.0301(3)	0.2804(2)	0.2499(3)	0.0170(5)	0.014(1)	0.019(1)	0.021(1)	−0.009(1)	−0.0068(8)	−0.0031(8)
Bi2	0.4696(3)	−0.2197(2)	0.2501(3)	0.0176(5)	0.015(1)	0.020(1)	0.021(1)	−0.010(1)	−0.0058(8)	−0.0044(8)
Tl1	0	½	½	0.0276(10)	0.034(1)	0.028(1)	0.027(3)	−0.016(2)	−0.008(1)	−0.006(1)
Tl2	½	0	½	0.0244(10)	0.011(1)	0.030(1)	0.035(3)	−0.015(2)	−0.005(1)	−0.005(1)
Tl3	½	½	0	0.0280(10)	0.036(2)	0.025(1)	0.027(3)	−0.009(1)	−0.012(1)	−0.006(1)
Tl4	0	0	0	0.0244(10)	0.012(1)	0.025(1)	0.035(3)	−0.009(1)	−0.010(1)	−0.004(1)
S1	0.043(1)	−0.108(1)	0.388(1)	0.013(2)						
S2	0.451(1)	0.116(1)	0.114(1)	0.007(2)						
S3	−0.460(1)	0.392(1)	0.384(1)	0.012(2)						
S4	−0.058(1)	0.619(1)	0.113(1)	0.016(3)						
O1	0.216(4)	−0.094(3)	0.416(3)	0.012(6)						
O2	−0.286(3)	0.395(3)	0.409(3)	0.009(5)						
O3	−0.161(4)	0.541(3)	0.090(3)	0.013(7)						
O4	0.335(3)	0.053(3)	0.087(3)	0.007(6)						
O5	0.557(5)	0.199(4)	−0.016(4)	0.029(9)						
O6	0.332(4)	0.200(3)	0.197(3)	0.018(6)						
O7	−0.183(4)	0.721(3)	0.180(3)	0.010(6)						
O8	−0.575(4)	0.531(3)	0.308(3)	0.011(6)						
O9	−0.073(4)	0.055(3)	0.310(3)	0.016(6)						
O10	0.112(4)	−0.195(3)	0.292(3)	0.015(6)						
O11	0.592(4)	0.015(3)	0.191(3)	0.014(6)						
O12	−0.396(5)	0.320(4)	0.300(4)	0.036(9)						
O13	−0.576(5)	0.327(4)	0.504(4)	0.038(9)						
O14	−0.087(3)	−0.191(3)	0.538(3)	0.011(5)						
O15	−0.058(4)	0.281(3)	0.032(3)	0.016(6)						
O16	0.083(4)	0.484(3)	0.209(3)	0.022(7)						

TABLE 5. Selected interatomic distances (Å) in markhininite.

Bi1–O9	2.27(3)	Tl3–O12	3.04(3) ×2
Bi1–O14	2.33(2)	Tl3–O16	3.16(3) ×2
Bi1–O16	2.37(3)	Tl3–O3	3.17(3) ×2
Bi1–O15	2.39(3)	Tl3–O5	3.18(3) ×2
Bi1–O6	2.49(3)	Tl3–O6	3.25(3) ×2
Bi1–O12	2.51(3)	Tl3–O8	3.30(3) ×2
Bi1–O2	2.51(2)	Tl3–O15	3.35(3) ×2
Bi1–O3	2.51(3)		
		Tl4–O10	3.01(3) ×2
Bi2–O7	2.38(2)	Tl4–O11	3.04(3) ×2
Bi2–O5	2.47(3)	Tl4–O15	3.06(3) ×2
Bi2–O10	2.47(2)	Tl4–O7	3.13(3) ×2
Bi2–O8	2.53(3)	Tl4–O4	3.19(3) ×2
Bi2–O13	2.58(3)	Tl4–O5	3.26(3) ×2
Bi2–O4	2.61(3)	Tl4–O9	3.47(3) ×2
Bi2–O1	2.63(3)		
Bi2–O11	2.65(3)	S1–O1	1.47(3)
		S1–O10	1.56(3)
Tl1–O16	3.04(3) ×2	S1–O14	1.57(3)
Tl1–O13	3.07(3) ×2	S1–O9	1.60(3)
Tl1–O10	3.13(3) ×2		
Tl1–O8	3.16(3) ×2	S2–O11	1.37(3)
Tl1–O2	3.25(3) ×2	S2–O5	1.37(4)
Tl1–O14	3.34(3) ×2	S2–O4	1.43(2)
Tl1–O7	3.50(3) ×2	S2–O6	1.45(3)
Tl2–O11	3.08(3) ×2	S3–O13	1.29(4)
Tl2–O14	3.09(2) ×2	S3–O12	1.34(4)
Tl2–O1	3.10(2) ×2	S3–O2	1.40(2)
Tl2–O9	3.21(2) ×2	S3–O8	1.43(3)
Tl2–O12	3.23(2) ×2		
Tl2–O6	3.28(2) ×2	S4–O3	1.45(3)
Tl2–O13	3.36(2) ×2	S4–O7	1.48(3)
		S4–O15	1.55(3)
		S4–O16	1.59(3)

(Shimoni-Livny *et al*., 1998). Holodirected coordination for Tl^{+} is much less preferable than hemidirected (with shorter and stronger Tl–O bonds concentrated in one coordination hemisphere) in oxysalt compounds. This feature of crystal chemical behaviour of Tl^{+} is influenced strongly by the degree of stereochemical activity of the so-called $6s^2$ lone electron pair. In order to evaluate the coordination environment of Tl^{+} cations in the structure of markhininite, ECC_v (volume eccentricity) eccentricity parameters (Makovicky and Balić-Žunić, 1998) were calculated using the computer program *IVTON* v.2 (Balić-Žunić and Vickovic, 1996). The ECC_v parameter is equal to zero for all four symmetrically independent Tl sites, which manifests the location of the Tl sites on inversion centres and, as a consequence, their highly symmetrical coordination.

Two symmetrically independent Bi atoms involve eight relatively strong Bi^{3+}–O bonds each (Fig. 5, Table 5) forming distorted tetragonal BiO_8 antiprisms. The coordination is rather symmetrical, which indicates a low degree of stereochemical activity of the so-called $6s^2$ lone electron pairs on the Bi^{3+} cations.

Four symmetrically independent S^{6+} cations form distorted SO_4 tetrahedra. The individual S–O distances are in the range 1.29–1.60 Å, which is outside the limits observed for well refined sulfate structures (1.394–1.578 Å; Hawthorne *et al*., 2000). Such dramatic variations would suggest substitution of S atoms by both smaller and larger cations, which should,

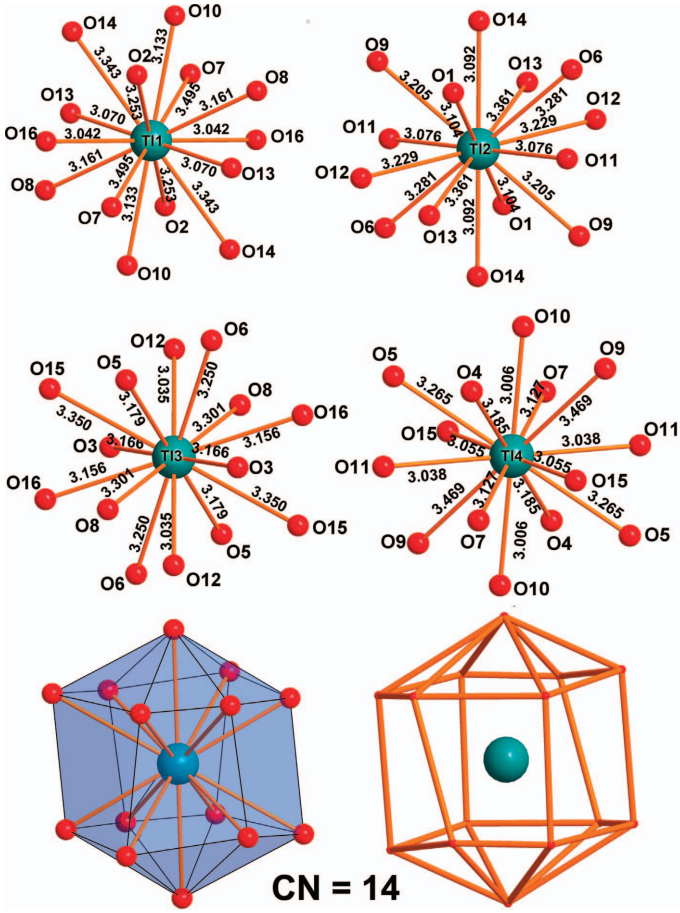

FIG. 4. Coordination of Tl^+ cations in markhininite. The coordination polyhedron of all thallium atoms can be represented as a combination of a hexagonal bipyramid and prism.

however, be excluded on the basis of electron microprobe chemical analyses. We believe that the deviations of the S–O bond lengths in the structure of markhininite from their typical values is due to the strong effects of twinning and Tl and Bi electron density dominance upon the results of crystal-structure refinement.

Structure description

BiO_8 tetragonal antiprisms and SO_4 tetrahedra share common O atoms to produce the $[Bi(SO_4)_2]^-$ layers parallel to (111) depicted in Fig. 6*b*. Figure 6*a* shows a black and white connectivity graph of the $[Bi(SO_4)_2]^-$ layer with the edges linking adjacent Bi (black) and S (white) vertices. The single and bold edges correspond to mono- and bidentate linkage modes between the cation polyhedra, respectively (Fig. 6*c*). Nodal representation of the $[Bi(SO_4)_2]^-$ layer in the structure of markhininite allows one to identify its relation to other minerals. $[M(TO_4)_2]^-$ layers (M = Fe, Mg; T = S, P) topologically similar to that observed in markhininite are known in the structures of yavapaiite, $KFe(SO_4)_2$ (Graeber and Rosenzweig, 1971), eldfellite, $NaFe(SO_4)_2$ (Balić-Žunić *et al.*, 2009) and brianite, $Na_2CaMg(PO_4)_2$ (Alkemper and Fuess, 1998).

The interlayer space in markhininite (Fig. 7) is filled by Tl^+ cations. The arrangement of the Tl atoms in the interlayer (Fig. 6*g*) is identical to that of the K atoms in the structure of yavapaiite (Fig. 6*h*) with a significant enlargement of the interatomic A–A (A = metal) distances due to the significantly larger ionic radius of the Tl^+ cation.

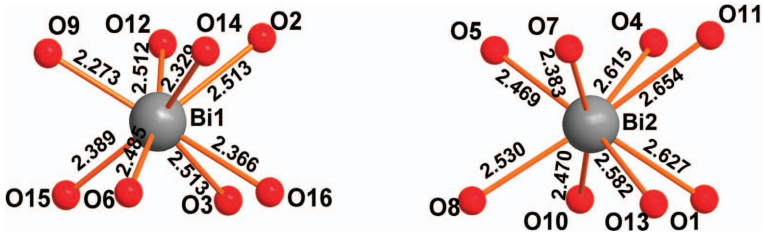

FIG. 5. Coordination of Bi^{3+} cations in markhininite.

Discussion

Markhininite is the first oxysalt compound containing both Tl and Bi. Its structure type is related to the yavapaiite-type compounds (Kolitsch *et al*., 2003). In fact, markhininite is one of few yavapaiite-type compounds that crystallize in a triclinic space group. The triclinic symmetry of the synthetic yavapaiite-type

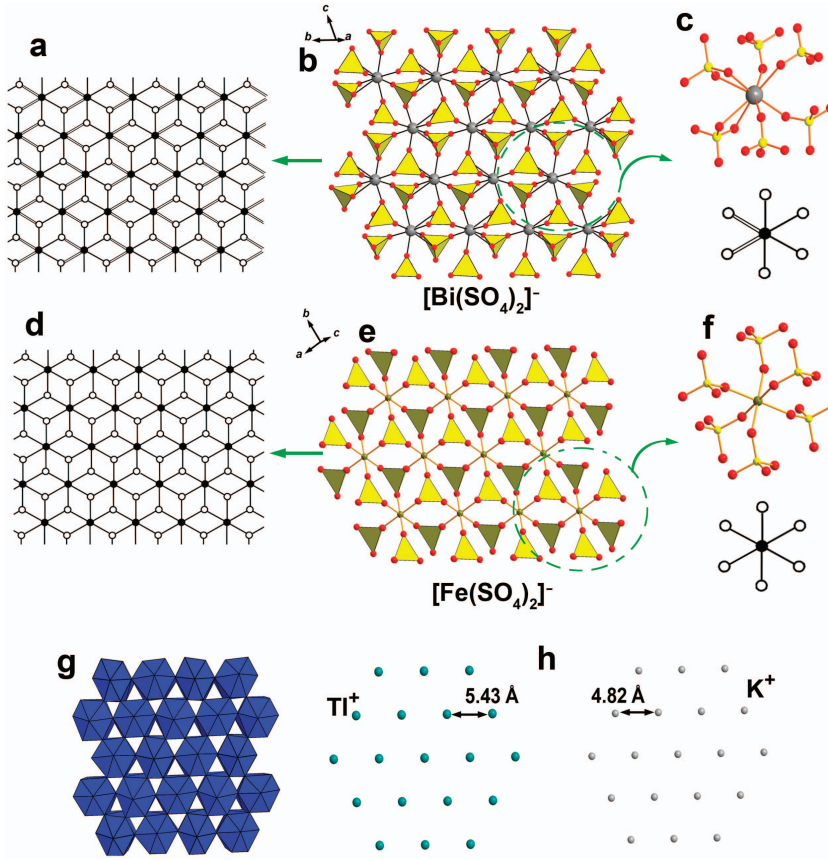

FIG. 6. Polyhedral representation of the $[Bi(SO_4)_2]^-$ layers in markhininite (*b*) and $[Fe(SO_4)_2]^-$ in yavapaiite (*e*) and their graphs (*a*, *d*). The bidentate linkage between the BiO_8 polyhedron and SO_4 tetrahedra in markhininite (*c*) and monodentate linkage between the FeO_6 and SO_4 in yavapaiite (*f*) are highlighted. A polyhedral representation of interlayer formed by TlO_{14} polyhedra (*g*) and comparison of Tl^+ cation packing in markhininite and K^+ packing in yavapaiite (*h*) is shown.

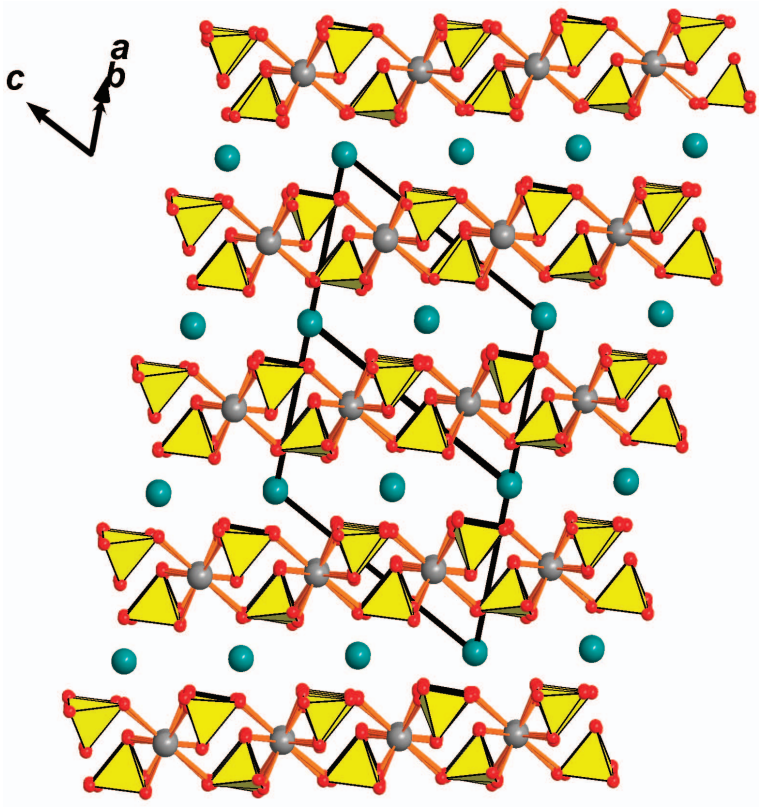

FIG. 7. General projection of the crystal structure of markhininite. SO_4 tetrahedra = yellow, and Bi^{3+} and Tl^{+} ions are shown as grey and cyan balls, respectively.

compound $KMn^{3+}[SeO_4]_2$ (Giester, 1995) was explained by the Jahn-Teller effect concerning octahedral Mn^{3+} coordination. In contrast to other yavapaiite-type compounds, which usually contain layers based upon corner-sharing octahedra and tetrahedra, BiO_8 polyhedra in markhininite share edges with adjacent SO_4 tetrahedra (Fig. 6). This bidentate type of linkage is usually avoided in the case of octahedrally coordinated cations such as Fe^{3+} in yavapaiite and eldfellite, due to electrostatic repulsive forces between cations in the second coordination sphere. However, the edge linkage may be favoured in the case of large and relatively low-charged cations such as rare earths and heavy *p*-elements. In fact, the $[Bi(SO_4)_2]^{-}$ layer in markhininite is virtually identical to that of the $[Eu(SO_4)_2]^{-}$ layer based upon SO_4 tetrahedra and EuO_8 tetragonal antiprisms in the crystal structure of $RbEu(SO_4)_2$ (Sarukhanyan *et al*., 1983; Krivovichev, 2009). In this context, it is remarkable that Tl^{+} and Bi^{3+} are often considered as relativistic alkali and rare-earth metals, respectively (Styszynski, 2010).

The Tl^{+} and Bi^{3+} coordination spheres in the structure of markhininite are relatively symmetrical, in good agreement with the observation that stereochemical activity of the so-called 'lone electron pairs' on heavy-metal cations (Tl^{+}, Pb^{2+}, Bi^{3+}) is more pronounced if their coordination environments contain strong Lewis bases (Krivovichev *et al*., 2013*b*). The Lewis basicity of the $(SO_4)^{2-}$ oxyanions is rather low (0.17 valence units (vu); calculated as a residual average bond valence of sulfate O atom, 0.5 vu, subdivided by three to keep the coordination number of O equal to four) (Hawthorne, 2012). Such a weak Lewis base as the sulfate O atom is unable to provide enough bond valence to distort the coordination environment of a Bi^{3+} cation, which needs Bi^{3+}–O bond valences of ~0.5 vu. However, 0.17 vu. is a high enough Lewis base strength to provide distortion of the oxygen coordination

environment of a Tl^{+} cation. Brown and Faggiani (1980) estimated the value of 0.22 vu as an approximate boundary for a Lewis base to be strong enough to favour stereochemical activity of the 'lone pairs' of electrons on a Tl^{+} cation. Below this boundary, the coordination environment of Tl^{+} may or may not be distorted, depending on the possibility of redistribution of bond valence. The value of 0.17 vu for an O^{2-} anion of a sulfate group is an average, and bond valence can be easily redistributed to provide Tl^{+}–O bonds of >0.20 vu. Thus, 'lone electron pairs' on Tl^{+} cations in sulfates may well be stereochemically active, as may be seen from the structures of karpovite and evdokimovite (Siidra *et al*., 2014*a*,*b*). However, in markhininite, the Lewis base strengths of sulfate oxyanions is modified sufficiently by formation of relatively strong Bi^{3+}–O bonds, which leaves little ability for O^{2-} anions to distort the coordination environment of Tl^{+}.

Due to its highly volatile behaviour, thallium can be transported easily by volcanic gases, resulting in high concentrations of Tl in fumarolic products relative to surrounding rocks. In Tolbachik fumaroles, this results in the formation of a suite of Tl sulfates, which are the subject of this series of papers. Markhininite, $TlBi(SO_4)_2$ is a new and unique mineral species and the first inorganic compound that contains both Tl and Bi. It has a new structure type, but is related to yavapaiite-type minerals and inorganic compounds. The discovery of markhininite thus significantly expands our knowledge of the mineralogy and geochemistry of thallium in volcanic fumarolic environments.

Acknowledgements

This work was supported by the Russian President grant K-3756.2014.5 (O.I.S.), the Russian Foundation for Basic Research (grant # 13-05-00684) and St Petersburg State University through the internal grants 3.38.83.2012 and 3.38.136.2014. Technical support by the SPbSU X-Ray Diffraction Resource Center is gratefully acknowledged.

References

Alkemper, J. and Fuess, H. (1998) The crystal structures of $NaMgPO_4$, $Na_2CaMg(PO_4)_2$ and $Na_{18}Ca_{13}Mg_5(PO_4)_{18}$: new examples for glaserite related structures. *Zeitschrift für Kristallographie*, **213**, 282–287.

Baker, R.G.A., Rehkämper, M., Hinkley, T.K., Nielsen, S.G. and Toutain, J.P. (2009) Investigation of thallium fluxes from subaerial volcanism – implications for the present and past mass balance of thallium in the oceans. *Geochimica et Cosmochimica Acta*, **73**, 6340–6359.

Balić-Žunić, T. and Vickovic, I. (1996) IVTON - program for the calculation of geometrical aspects of crystal structures and some crystal chemical applications. *Journal of Applied Crystallography*, **29**, 305–306.

Balić-Žunić, T., Moelo, Y., Loncar, Z. and Micheelsen, H. (1994) Dorallcharite, $Tl_{0.8}K_{0.2}Fe_3(SO_4)_2(OH)_6$, a new member of the jarosite-alunite family. *European Journal of Mineralogy*, **6**, 255–263.

Balić-Žunić, T., Garavelli, A., Acquafredda, P., Leonardsen, E. and Jakobsson, S.P. (2009) Eldfellite, $NaFe(SO_4)_2$, a new fumarolic mineral from Eldfell volcano, Iceland. *Mineralogical Magazine*, **73**, 51–57.

Brown, I.D. and Faggiani, R. (1980) The structure of thallium(I) tetraacetatothallate(III): when is the lone pair of electrons on Tl^{I} stereoactive? *Acta Crystallographica*, **B36**, 1802–1806.

Campostrini, I., Demartin, F. and Gramaccioli, C.M. (2008) Hephaistosite, $TlPb_2Cl_5$ a new mineral species from La Fossa crater, Vulcano, Aeolian Islands, Italy. *The Canadian Mineralogist*, **46**, 701–708.

CNMNC (2013) IMA list of minerals. http://pubsite-s.uws.edu.au/ima-cnmnc/ [Accessed on 15/07/2013].

Daiyan, C., Guanxin, W., Zhenxi, Z. and Yuming, C. (2001) A new mineral – lanmuchangite. *Acta Mineralogica Sinica*, **21**, 271–277.

Demartin, F., Gramaccioli, C.M. and Campostrini, I. (2009) Steropesite, Tl_3BiCl_6, a new thallium bismuth chloride from La Fossa crater, Vulcano, Aeolian islands, Italy. *The Canadian Mineralogist*, **47**, 373–380.

Fedotov, S.A. (editor) (1984) *Large Tolbachik Fissure Eruption. Kamchatka 1975–1976*. Nauka, Moscow.

Fedotov, S.A. and Markhinin, Y.K. (editors) (2011) *The Great Tolbachik Fissure Eruption: Geological and Geophysical Data 1975–1976*. Cambridge University Press, Cambridge, UK.

Filatov, S.K., Vergasova, L.P., Siidra, O.I., Krivovichev, S.V. and Kretser, Y.L. (2013) Markhininite, IMA 2012-040. CNMNC Newsletter No. 15, February 2013, page 2; *Mineralogical Magazine*, **77**, 1–12. IMA No. 2012-045.

Giester, G. (1995) Crystal structure of $KMn^{3+}(SeO_4)_2$ – a triclinic distorted member of the yavapaiite family. *Mineralogy and Petrology*, **53**, 165–171.

Graeber, E.J. and Rosenzweig, A. (1971) The crystal structures of yavapaiite, $KFe(SO_4)_2$, and goldichite,

$KFe(SO_4)_2(H_2O)_4$. *American Mineralogist*, **56**, 1917–1933.

Hawthorne, F.C. (2012) A bond-topological approach to theoretical mineralogy: crystal structure, chemical composition and chemical reactions. *Physics and Chemistry of Minerals*, **39**, 841–874.

Hawthorne, F.C., Krivovichev, S.V. and Burns, P.C. (2000) The crystal chemistry of sulfate minerals. Pp. 1–112 in: *Sulfate Minerals: Crystallography, Geochemistry, and Environmental Significance* (C.N. Alpers, J.L. Jambor and D.K. Nordstrom, editors). Reviews in Mineralogy and Geochemistry, **40**. Mineralogical Society of America and the Geochemical Society, Washington, DC.

Johan, Z. and Mantienne, J. (2000) Thallium-rich mineralization at Jas Roux, Hautes-Alpes, France: a complex epithermal, sediment-hosted, ore-forming system. *Journal of the Czech Geological Society*, **45**, 63–77.

Karup-Møller, S. and Makovicky, E. (2011) Mineral X, a new thalcusite homologue from the Ilímaussaq complex, South Greenland. *Bulletin of the Geological Society of Denmark*, **59**, 13–22.

Kellerhals, T., Tobler, L., Brütsch, S., Sigl, M., Wacker, L., Gäggeler, H.W. and Schwikowski, M. (2010) Thallium as tracer for preindustrial volcanic eruptions in the ice core record from Illimani, Bolivia. *Environmental Science & Technology*, **44**, 888–893.

Kolitsch, U., Maczka, J. and Hanuza, J. (2003) $NaAl(MoO_4)_2$: a rare structure type among layered yavapaiite-related $AM(XO_4)_2$ compounds. *Acta Crystallographica*, **E59**, i10–i13.

Kovalenker, V.A., Laputina, I.P., Evstigneeva, T.L. and Izoitko, V.M. (1976) Thalcusite $Cu_{3-x}Tl_2Fe_{1+x}S_4$ new sulphide of thallium from coppernickel ores of the Talnakh deposit. *Zapiski Vsesoyuznogo Mineralogicheskogo Obshchestva*, **105**, 202–206.

Krivovichev, S.V. (2009) *Structural Crystallography of Inorganic Oxysalts*. Oxford University Press, Oxford, UK.

Krivovichev, S.V., Vergasova, L.P., Filatov, S.K., Rybin, D.S., Britvin, S.N. and Ananiev, V.V. (2013*a*) Hatertite, $Na_2(Ca, Na)(Fe^{3+}, Cu)_2(AsO_4)_3$, a new alluaudite-group mineral from Tolbachik fumaroles, Kamchatka peninsula, Russia. *European Journal of Mineralogy*, **25**, 683–691.

Krivovichev, S.V., Mentré, O., Siidra, O.I., Colmont, M. and Filatov, S.K. (2013*b*) Anion-centered tetrahedra in inorganic compounds. *Chemical Reviews*, **113**, 6459–6535.

Li, Y.-H. and Schoonmaker, J.E. (2003) Chemical composition and mineralogy of marine sediments. Pp. 1–35 in: *Treatise on Geochemistry, Vol. 7. Sediments, Diagenesis, and Sedimentary Rocks* (F.T. Mackenzie, editor). Elsevier-Pergamon, Oxford, UK.

Makovicky, E. and Balić-Žunić, T. (1998) New measure of distortion for coordination polyhedra. *Acta Crystallographica*, **B54**, 766–773.

Markhinin, E.K. (1967) *The Role of Volcanism in Formation of the Earth's Crust*. Nauka, Moscow.

Murashko, M.N., Pekov, I.V., Krivovichev, S.V., Chernyatyeva, A.P., Yapaskurt, V.O., Zadov, A.E. and Zelensky, M.E. (2013) Steklite, $KAl(SO_4)_2$: a finding at the Tolbachik Volcano, Kamchatka, Russia, validating its status as a mineral species and crystal structure. *Geology of Ore Deposits*, **55**, 594–600.

Naboko, S.I. and Glavatskikh, S.F. (1984) Post-eruption process. Pp. 309–340 in: *Large Tolbachik Fissure Eruption. Kamchatka 1975–1976* (S.A. Fedotov, editor). Nauka, Moscow.

Palme, H. and O'Neill, H.St.C. (2003) Cosmochemical estimates of mantle composition. Pp. 1–38 in: *Treatise on Geochemistry, Vol. 2. The Mantle and Core* (R.W. Carlson, editor). Elsevier-Pergamon, Oxford, UK.

Pekov, I.V., Zelenski, M.E., Zubkova, N.V., Ksenofontov, D.A., Kabalov, Y.K., Chukanov, N.V., Yapaskurt, V.O., Zadov, A.E. and Pushcharovsky, D.Y. (2012*a*) Krasheninnikovite, $KNa_2CaMg(SO_4)_3F$, a new mineral from the Tolbachik volcano, Kamchatka, Russia. *American Mineralogist*, **97**, 1788–1795.

Pekov, I.V., Zelenski, M.E., Zubkova, N.V., Yapaskurt, V.O., Chukanov, N.V., Belakovskiy, D.I. and Pushcharovsky, D.Y. (2012*b*) Calciolangbeinite, $K_2Ca_2(SO_4)_3$, a new mineral from the Tolbachik volcano, Kamchatka, Russia. *Mineralogical Magazine*, **76**, 673–682.

Pekov, I.V., Zelenski, M.E., Yapaskurt, V.O., Polekhovsky, Y.S. and Murashko, M.N. (2013*a*) Starovaite, $KCu_5O(VO_4)_3$, a new mineral from fumarole sublimates of the Tolbachik volcano, Kamchatka, Russia. *European Journal of Mineralogy*, **25**, 91–96.

Pekov, I.V., Zubkova, N.V., Zelenski, M.E., Yapaskurt, V.O., Polekhovsky, Y.S., Fadeeva, O.A. and Pushcharovsky, D.Y. (2013*b*) Yaroshevskite, $Cu_9O_2(VO_4)_4Cl_2$, a new mineral from the Tolbachik volcano, Kamchatka, Russia. *Mineralogical Magazine*, **77**, 107–116.

Prytulak, J., Nielsen, S.G., Plank, T., Barker, M. and Elliott, T. (2013) Assessing the utility of thallium and thallium isotopes for tracing subduction zone inputs to the Mariana arc. *Chemical Geology*, **345**, 139–149.

Roberts, A.C., Venance, K.E., Seward, T.M., Grice, J.D. and Paar, W.H. (2006) Lafossaite, a new mineral from the La Fossa Crater, Vulcano, Italy. *Mineralogical Record*, **37**, 165–168.

Rudnick, R.L. and Gao, S. (2003) The composition of the continental crust. Pp. 1–64 in: *Treatise on*

Geochemistry, Vol. 3. The Crust (R.L. Rudnick, editor). Elsevier-Pergamon, Oxford, UK.

Sarukhanyan, N.L., Iskhakova, L.D. and Trunov, V.K. (1983) Crystal structure of $RbEu(SO_4)_2$. *Kristallografiya*, **28**, 452–456.

Shimoni-Livny, L., Glusker, J.P. and Bock, C.W. (1998) Lone pair functionality in divalent lead compounds. *Inorganic Chemistry*, **37**, 1853–1867.

Shuvalov, R.R., Vergasova, L.P., Semenova, T.F., Filatov, S.K., Krivovichev, S.V., Siidra, O.I. and Rudashevsky, N.S. (2013) Prewittite, $KPb_{1.5}Cu_6Zn(SeO_3)_2O_2Cl_{10}$, a new mineral from Tolbachik Fumaroles, Kamchatka Peninsula, Russia: description and crystal structure. *American Mineralogist*, **98**, 463–469.

Siidra, O.I., Vergasova, L.P., Kretser, Y.L., Polekhovsky, Y.S., Filatov, S.K. and Krivovichev, S.V. (2014*a*) Unique thallium mineralization in the fumaroles of Tolbachik volcano, Kamchatka Peninsula, Russia. II. Karpovite, $Tl_2VO(SO_4)_2(H_2O)$. *Mineralogical Magazine*, **78**, 1699–1709.

Siidra, O.I., Vergasova, L.P., Kretser, Y.L., Polekhovsky, Y.S., Filatov, S.K. and Krivovichev, S.V. (2014*b*) Unique thallium mineralization in the fumaroles of Tolbachik volcano, Kamchatka Peninsula, Russia. III. Evdokimovite, $Tl_4(VO)_3(SO_4)_5(H_2O)_5$. *Mineralogical Magazine*, **78**, 1711–1724.

Speck, A.L. (2003) Single-crystal structure validation with the program *PLATON*. *Journal of Applied Crystallography*, **36**, 7–13.

Starova, G.L., Vergasova, L.P., Filatov, S.K., Britvin, S.N. and Anan'ev, V.V. (2012) Lammerite-β, $Cu_3(AsO_4)_2$, a new mineral from fumaroles of the Great Fissure Tolbachik eruption, Kamchatka Peninsula, Russia. *Geology of Ore Deposits*, **54**, 565–569.

Styszynski, J. (2010) Challenges and advances in computational chemistry and physics. Pp. 99–164 in: *Relativistic Methods for Chemists Vol. 10* (M. Barysz and J. Ishikawa, editors). Springer, Dordrecht, The Netherlands.

Zelenski, M.E., Zubkova, N.V., Pekov, I.V., Boldyreva, M.M., Pushcharovsky, D.Y. and Nekrasov, A.N. (2011) Pseudolyonsite, $Cu_3(VO_4)_2$, a new mineral species from the Tolbachik volcano, Kamchatka Peninsula, Russia. *European Journal of Mineralogy*, **23**, 475–481.

Zelenski, M.E., Zubkova, N.V., Pekov, I.V., Polekhovsky, Y.S. and Pushcharovsky, D.Y. (2012) Cupromolybdite, $Cu_3O(MoO_4)_2$, a new fumarolic mineral from the Tolbachik volcano, Kamchatka Peninsula, Russia. *European Journal of Mineralogy*, **24**, 749–757.